A New Interpretation of the Structure of the Mycolyl−Arabinogalactan Complex of *Mycobacterium tuberculosis* As Revealed through Characterization of Oligoglycosylalditol Fragments by Fast-Atom Bombardment Mass Spectrometry and ^{1}H Nuclear Magnetic Resonance Spectroscopy†

Gurdyal S. Besra,*,‡ Kay-Hooi Khoo,§ Michael R. McNeil,‡ Anne Dell,§ Howard R. Morris,§ and Patrick J. Brennan‡

Department of Microbiology, Colorado State University, Fort Collins, Colorado 80523, and Department of Biochemistry, Imperial College of Science, Technology, and Medicine, London SW7 2AZ, U.K.

Received September 29, 1994; Revised Manuscript Received January 6, 1995®

ABSTRACT: Previous structural analysis of small oligosaccharide fragments had allowed the recognition of several small structural motifs within arabinogalactan, the dominant cell wall structural polysaccharide of *Mycobacterium tuberculosis*. To determine how these motifs are connected to one another to form the complete polymer, oligosaccharide fragments containing up to 26 glycosyl residues were released by gentle acid hydrolysis of the per-*O*-methylated arabinogalactan, converted to fully per-*O*-alkylated oligoglycosylalditols, and purified by high-performance liquid chromatography, and the molecular weights and alkylation patterns of the resultant oligoglycosyl fragments were determined by fast atom bombardment mass spectrometry. The results, combined with previous studies, allowed further understanding of the intricate structural features of the nonreducing ends of arabinogalactan. Thus, the extended nonreducing ends of the arabinan were shown to consist of a tricosaarabinoside (23-mer). We reason that three such arabinan motifs are attached to the homogalactan component of arabinogalactan, which was previously shown to consist of alternating 5- and 6-linked β-D-galactofuranosyl residues. Using the same approach as applied to the arabinan branches, an extended stretch of the galactan was isolated that consisted of at least 23 alternating β-1,6 and β-1,5 D-Gal*f* residues, devoid of any branching, demonstrating that the points of attachment of the arabinan chains to galactan are close to the reducing end of galactan, which itself is linked to peptidoglycan via the linker disaccharide phosphate L-Rha*p*-(1→3)-α-D-GlcNAc-P. By nuclear magnetic resonance analysis, the L-Rha*p* was shown to be in the α configuration. The long-chain α-alkyl-β-hydroxy mycolic acids, known to occupy the 5-positions of both the terminal β-D-Ara*f* and internal 2-α-D-Ara*f* residues of the terminal branched pentaarabinosyl motif, are now shown to be nonacylated at the β-hydroxy function. Lack of acylation points to intramolecular hydrogen bonding between the β-hydroxyl and carbonyl functions of the mycolic acid, providing a highly ordered arrangement of mycolic acids in accord with evolving models of the orientation of the cell wall polymers in mycobacterial cell walls. A revised model is proposed for the composition and orientation of the mycolyl−arabinogalactan in the cell walls of *M. tuberculosis*, which should increase our understanding of cell wall hydrophobicity, impermeability, and role in disease pathogenesis.

Structurally, mycobacterial cell walls incorporate features of both Gram-positive and Gram-negative bacteria as well as displaying more specialized components. In common with cell walls of other actinomycetes and coryneform bacteria, the mycobacterial cell wall is dominated by a nonrepeating polysaccharide, arabinogalactan (AG),[1] constituting about 35% of the cell wall mass. This polymer is covalently bound at the reducing end through a "linker" disaccharide phosphate, L-Rha*p*-(1→3)-D-GlcNAc-P, to a chemotype IV peptidoglycan (Azuma et al., 1974; Draper, 1982; Petit & Lederer, 1984; McNeil et al., 1990). The nonreducing end of the arabinan is esterified by long-chain α-alkyl-β-hydroxy fatty acids, the mycolic acids (Amar-Nacasch & Vilkas, 1970; Azuma et al., 1968). Recently, a more detailed structural interpretation of the mycolyl−arabinogalactan (mAG) complex was made possible with the recognition of a few distinct arabinofuranosyl- (Ara*f*-) and galactofuranosyl-

† Supported by the National Institute of Allergy and Infectious Diseases, National Institutes of Health (Grant AI-18357 to P.J.B.), a Medical Research Council (U.K.) Program Grant (to H.R.M. and A.D.), a Wellcome Trust Prize Studentship (to K.-H.K.), and a postdoctoral fellowship from the Heiser Program for Research in Leprosy and Tuberculosis (to G.S.B.) The NMR conducted at the Colorado State University Regional NMR Center was supported by National Science Foundation Grant CHE 86-16437.

* To whom correspondence should be addressed.

‡ Colorado State University.

§ Imperial College of Science, Technology, and Medicine.

® Abstract published in *Advance ACS Abstracts,* March 15, 1995.

[1] Abbreviations: AG, arabinogalactan; mAGP, mycolyl−arabinogalactan−peptidoglycan complex; Ac, acetyl; Ara, arabinosyl; *f*, furanosyl; Gal, galactosyl; Me, methyl; Rha, rhamnosyl; *p*, pyranosyl; t, terminal; SDS, sodium dodecyl sulfate; TFA, trifluoroacetic acid; BCG, Bacille Calmette-Guerin; TMC, Trudeau mycobacterial collection; TLC, thin-layer chromatography; GC/MS, gas chromatography−mass spectrometry; EI/MS, electron impact mass spectrometry; HPLC, high-performance liquid chromatography; FAB/MS, fast atom bombardment mass spectrometry; GlcNAc, *N*-acetylglucosamine; NMR, nuclear magnetic resonance; 2D COSY, two-dimensional chemical shift correlated spectroscopy.

0006-2960/95/0434-4257$09.00/0

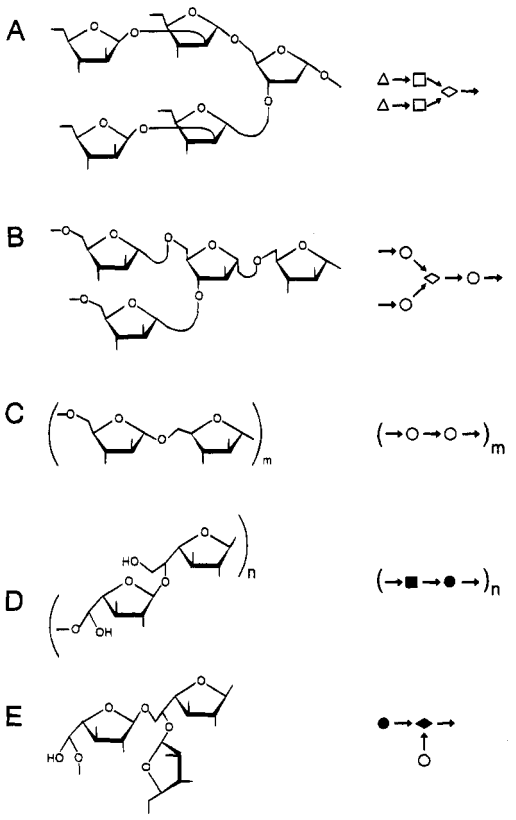

FIGURE 1: Representation of the five major structural motifs that represent *M. tuberculosis* AG as shown previously (Daffe et al., 1990).

(Gal*f*-) containing structural motifs (Figure 1) (Daffe et al., 1990). The nonreducing termini of arabinan consist of pentaarabinosyl motifs [β-D-Ara*f*-(1→2)-α-D-Ara*f*]$_2$-(3 and 5)-α-D-Ara*f* attached through a linear stretch of α-5-linked D-Ara*f* and some branched α-3,5-linked D-Ara*f* units to the galactan. About two-thirds of these pentaarabinosyl termini are esterified with four mycolic acid residues at the 5-position of both the terminal β-D-Ara*f* and internal 2-linked α-D-Ara*f* units. The basic structure of the mycolic acids can be represented by the formula $R_1CH(OH)CH(R_2)COOH$, where R_2 is a $C_{20}-C_{24}$ alkyl chain and R_1 is a complex structure of about 60−70 carbon atoms containing rather unusual functions, such as cyclopropane rings, double bonds, methyl branches, and methoxy, hydroxy, and keto functions. The galactan is known to consist of between 10 and 20 units of [→6-β-D-Gal*f*-(1→5)-β-D-Gal*f*(1→]$_2$. However, the ways in which these constituent motifs are assembled to form the mature heteropolysaccharide were unknown; a speculative model incorporating these motifs have been published (Daffe et al., 1990; McNeil et al., 1991). The recognition of these primary structural motifs has fueled speculation and experiment concerning the special arrangement of components of the mAGP complex and their contribution to cell wall impermeability (Nikaido et al., 1993).

In this present study, fast atom bombardment mass spectrometry (FAB/MS) analyses of much larger per-*O*-alkylated oligosaccharide alditol fragments allowed us to amalgamate several of the known motifs into large tricosaarabinoside arrangements and to suggest the points of linkage of these to the galactan core. Also, the question of the orientation of the α-branched-β-hydroxy mycolic acids on the terminal reaches of this arabinoside was addressed, allowing the formulation of a model of highly ordered, oriented mycolic acids on the key tricosaarabinosides.

EXPERIMENTAL PROCEDURES

Growth of Organisms and Isolation of the mAGP Complex. *Mycobacterium bovis* BCG (Danish strain Lilly) was obtained in the lyophilized form from S. D. Chaparas (Bureau of Biologics, Food and Drug Administration, Bethesda, MD). *Mycobacterium tuberculosis* Erdman (TMC 107) and *M. bovis* were grown on 7H11 broth for 2−3 weeks at 37 °C. *Mycobacterium leprae* was obtained from armadillo livers and spleens as described recently (Pessolani et al., 1993). All mycobacterial suspensions were autoclaved and the cells were recovered by centrifugation, washed, and frozen at −20 °C. The thawed bacterial cells were resuspended in phosphate buffer containing 2% Triton X-100 (pH 7.2), disrupted by sonication, and centrifuged at 27000*g* (Daffe et al., 1990). The pelleted material was extracted three times with 2% (w/v) SDS in phosphate buffer at 95 °C for 1 h to remove associated proteins, successively washed with water, 80% (v/v) acetone in water, and acetone, and finally lyophilized to yield a highly purified cell wall preparation rich in mycolic acids, arabinogalactan, and peptidoglycan (Hirschfield et al., 1990), i.e., the mAGP complex (Hirschfield et al., 1990).

Methylation and Depolymerization of Arabinogalactan. Insoluble cell walls from *M. tuberculosis* Erdman (TMC 107) (100 mg) were methylated by a modification of the Hakomori procedure using CH_3I as described (McNeil et al., 1990; Hakomori, 1964), which also served to cleave the mycolyl esters and most of the peptidoglycan. The resultant acetone-soluble per-*O*-methylated arabinogalactan (30 mg) was subjected to partial acid hydrolysis in 3-mg aliquots in 200 μL of 2 M TFA for 40 min at 60 °C. Hydrolysates were combined, reduced with $NaB[^2H]_4$, and either per-*O*-trideuteriomethylated or per-*O*-ethylated according to the Hakomori alkylating procedure. Reaction products were removed from the mixture of per-*O*-alkylated oligoglycosylalditols on a C-18 Sep-Pak cartridge (Waters, Milford, MA) as described (Daffe et al., 1990).

Alternative Methylation To Preserve Mycolyl Functions. Cell walls from *M. tuberculosis* Erdman (TMC 107), *M. bovis* BCG, *M. avium*, and *M. leprae* were methylated under the neutral methyltrifluoromethane sulfonate conditions (Prehm, 1980) which served to retain the mycolyl functions. Cell walls (10 mg) were suspended in 2 mL of trimethyl phosphate (Aldrich Chemical Co., Milwaukee, WI) followed by the addition of 600 μL of 2,6-di-*tert*-butylpyridine and 200 μL of methyltrifluoromethane sulfonate (both from Aldrich). The reaction mixture was stirred for 6 h at 50 °C, neutralized with pyridine, dialyzed, and freeze-dried to yield the per-*O*-methylated mAGP complex. To release the mycolic acids, either the original mAGP or the per-*O*-methylated mAGP (5 mg) was suspended in 15% tetrabutylammonium hydroxide (1 mL) and heated at 100 °C overnight (Dobson et al., 1985). After cooling, H_2O (1 mL), followed by CH_2Cl_2 (2 mL) and an excess of CH_3I (100 μL), was added and the reaction mixture was stirred for 1 h. Two milliliters of 1 M HCl was added, the sample was vortexed and centrifuged, and the upper phase was discarded. The lower organic layer was washed with H_2O (2 mL), evaporated to dryness, and examined by TLC for mycolate methyl esters or per-*O*-methylated mycolate after multiple develop-

ments in petroleum ether/diethyl ether (95:5). Separated components were revealed by spraying with ethanolic molybdophosphoric acid and heating at 110 °C for 15 min. Individual per-*O*-methylated mycolate methyl esters of the α, methoxy, and keto designations were subjected to preparative TLC on 10- × 10-cm Merck 5735 plastic-coated sheets in the same solvent. Separated components were detected with 0.01% ethanolic rhodamine 6G, scraped from the sheets, and extracted with diethyl ether to afford the three families of purified per-*O*-methylated mycolate methyl esters.

HPLC Separation and GC/MS Analysis of Per-O-Alkylated Oligoglycosylalditols. The mixture of per-*O*-alkylated oligoglycosylalditols (10−15 mg) arising from the depolymarization step was dissolved in aqueous 40% CH_3CN and injected onto a 0.4- × 25-cm Hibar RP-18 reversed-phase column (EM Science, Gibbstown, NJ) connected to a Beckman Model 110A HPLC (Beckman, San Ramon, CA). The solvent gradient involved 1 min of aqueous 40% CH_3CN followed by a linear gradient to 100% CH_3CN for 60 min and a final 10-min hold at 100% CH_3CN. The flow rate was 1 mL/min. Fractions (1 mL) were collected, dried, and analyzed by GC/MS and FAB/MS or, alternatively, hydrolyzed, reduced, and per-*O*-acetylated as described (McNeil et al., 1990); all drying steps were conducted at room temperature to avoid evaporative loss of the volatile, highly alkylated alditols. For purposes of determining sugar content and linkage patterns, such samples were analyzed by GC/MS using a Hewlett-Packard 5890 gas chroamtograph connected to a Hewlett-Packard 5970 mass selective detector as described (McNeil et al., 1990; Besra et al., 1991).

Isolation of the Per-O-Methylated Oligoglycosylalditol "Linker Fragments". mAGP (2.0 g) from *M. bovis* BCG was partially hydrolyzed with 0.2 M H_2SO_4 (100 mL) at 100 °C for 30 min, neutralized with barium carbonate, filtered, and concentrated, and the residue was redissolved in 1 M NH_4OH (10 mL) and reduced with 200 mg $NaBH_4$ as described by Fujioko et al. (1985). After acidification with acetic acid, the mixture was applied to a column of Dowex 50W × 8 (H^+ form, 2 × 20 cm), eluted with H_2O (250 mL), and concentrated; boric acid was removed by codistillation with methanol, and the resulting oligoglycosylalditols were per-*O*-methylated (Hakormori, 1964). The reaction mixture was poured into H_2O (100 mL) and extracted four times with $CHCl_3$ (50 mL). The combined $CHCl_3$ extracts were dried over anhydrous $MgSO_4$, filtered, and concentrated. The per-*O*-methylated products were applied to a Florisil column (1 × 100 cm) and eluted stepwise with 100 mL of $CHCl_3$ followed by 250 mL of 2% and 5% CH_3OH in $CHCl_3$. Fractions (10 mL) were collected and analyzed by TLC in $CHCl_3/CH_3OH$ (95:5) after spraying with 10% sulfuric acid in ethanol and heating at 110 °C for 5 min. Carbohydrate-containing fractions were pooled, applied to a reverse-phase C-18 Sep-Pak cartridge (Waters, Milford, MA), and eluted stepwise with 6 mL of 5%, 10%, 20%, 30%, 40%, and 50% CH_3CN in H_2O, and fractions (2 mL) were analyzed by GC/MS. A standard of α- and β-tri-*O*-methylrhamnose methyl glycosides was prepared from monomeric rhamnose according to the procedure of Ciucanu and Kerek (1984).

NMR and FAB/MS Analyses. NMR was performed on a Bruker ACE-300 instrument at the Colorado State University Department of Chemistry Central Instrument Facility. ^1H and 2D COSY NMR spectra were obtained for the per-*O*-methylated oligoglycosylalditol derivative of L-Rha*p*-(1→3)-D-GlcNAc at a concentration of 0.9 mg/0.5 mL of $C[^2H]_3Cl$ (Besra et al., 1992). Additionally, spectra were obtained for purified per-*O*-methylated α-, methoxy-, and ketomycolate methyl esters at a concentration of 0.5 mg/0.5 mL of $C[^2H]_3Cl$. Acetone was added to the samples and its signal was assigned to 2.225 ppm for ^1H NMR and 31.40 ppm for ^{13}C NMR, which corresponds to δ 0 for tetramethylsilane. Inverse detection probe was used to perform ^1H-detected 2D [$^{13}C-^1H$] shift correlation (HMQC) experiments as described (Bax & Summers, 1986). FAB/MS of per-*O*-alkylated oligoglycosylalditol products were obtained on a VG Analytical ZAB HF mass spectrometer equipped with a M-Scan FAB gun operating at 10 kV and 20 μA and using xenon as the bombarding gas as described (Dell, 1990). Spectra were recorded on UV-sensitive oscillographic paper and were counted manually. Samples were dissolved in CH_3OH and loaded onto a matrix of *m*-nitrobenzyl alcohol.

RESULTS

Strategy for the Generation and Analysis of Per-O-Alkylated Oligoglycosylalditols. The structural elucidation of a complex polysaccharide such as AG which lacks a repeating unit is difficult and is often not amenable to analysis by modern analytical methods such as multidimensional NMR. Instead, analysis invariably involves characterization of partial degradative products leading to deduction of the structure of the native polymer. An earlier strategy of ours toward deducing the structure of the pivotal arabinogalactan of mycobacterial cell walls (Daffe et al., 1990) involved partial acid hydrolysis of the per-*O*-methylated AG, reduction, per-*O*-pentadeuterioethylation, separation by reverse-phase HPLC, and structural determination by ^1H NMR and GC/MS of the resulting per-*O*-alkylated oligoglycosylalditol fragments (up to triglycosylalditols or "4-mers"). Elucidation of the structures of many such fragments allowed the recognition of five dominant motifs within arabinogalactan (Figure 1).

We hypothesized that further definition of the interarrangement of these motifs could be achieved by even milder acid hydrolysis to generate larger fragments beyond the range of analysis by GC/MS but amenable to FAB/MS. The application of this approach to the arabinan and galactan segments of the heteropolysaccharide is shown in Figures 2 and 3, respectively. Note that the number of cleavages or "clips" necessary to generate a given per-*O*-alkylated oligoglycosylalditol is readily determined by the number of added $C[^2H]_3$ groups. Thus, as shown in Figure 2A, an arabinan fragment produced by a single cleavage (a one-clip arabinan) contains only the two $C[^2H]_3$ groups on the reducing alditol. Such one-clip arabinans must come from the nonreducing end of the arabinan component of the heteropolysaccharide. In contrast, an arabinan fragment formed by two clips has an additional $C[^2H]_3$ group (Figure 2B). Moreover, knowledge of the mere molecular weight of one-clip fragments generated from the reducing end of AG in combination with our previous studies should allow the entire structure of such a fragment to be deduced. On the other hand, fragments arising from two or more clips can be generated in a number of ways and, in the case of those arising from arabinan segments, can be only partially defined and are of more limited usefulness in terms of structural interpretations.

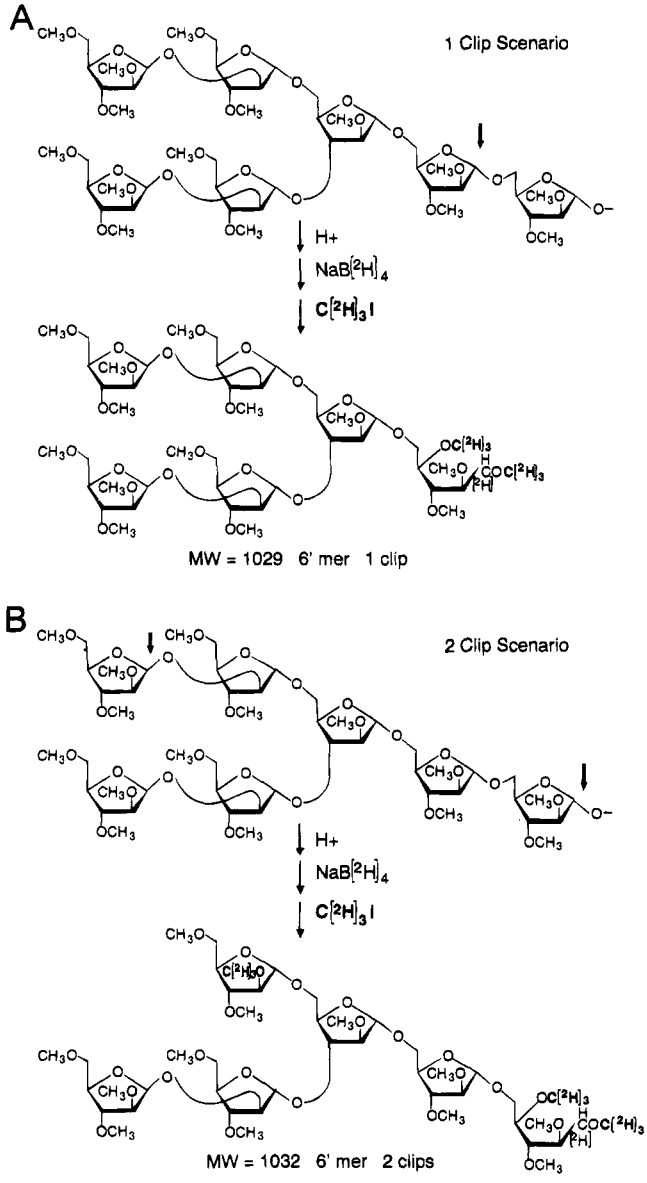

FIGURE 2: Formation of alkylated pentaarabinosylarabinitols (6-mers) by one (A) or two cleavages (B). Only a single structure can be produced by one cleavage (panel A), whereas multiple structures can be produced by two cleavages. Only one example of such a cleavage is shown in panel B. With $C[^2H]_3$ labeling, the products produced by two cleavages weigh 3 mass units more than those produced by a single cleavage.

Analysis of the Per-O-Methylated, Per-O-Trideuteriomethylated Oligoglycosylalditol Fragments. The mixture of large per-*O*-alkylated oligoglycosylalditols arising from gentle hydrolysis of the AG portion of mAGP was subjected to reverse-phase HPLC, from which collected fractions were analyzed by FAB/MS. Screening of the fractions for the trideuteriomethyl "tag" resulted in the recognition of a number of key fragments (Table 1). These are represented in terms of the number of Ara or Gal residues and the number of clips responsible for their production. First, focusing on Ara-containing fragments, major signals corresponding to Ara_{6-8} arising from one clip were found in fractions 10−16. However, $Ara_{9,10}$ fragments produced by a single clip, although present in fractions 17−18, were much less abundant than the corresponding two-clip $Ara_{9,10}$ fragments. In addition, Ara-containing fragments produced by a single clip and containing 11−16 residues (one-clip Ara_{11-16}) were not found in detectable amounts (Table 1). Dramatically, however, an ion corresponding to one-clip Ara_{17} at *m/z* 2812 appeared in fraction 29 (Table 1 and Figure 4). Additional fragments corresponding to one-clip Ara_{18-22} were found in later fractions. This loss of nonreducing-terminal Ara-containing fragments with nine residues and the reappearance of such fragments with 17 units provided important clues as to how motifs A, B, and C (Figure 1) are combined with each other to provide an Ara_{23} fragment. A macromotif encompassing the nonreducing end of arabinan is in Figure 5A. In accord with the evidence, macromotif A can form one-clip Ara_8 and Ara_{17-23} but not one-clip Ara_{9-16}.

Second, concerning the Gal-containing fragments, intense signals indicative of sizable cleavage fragments were observed. In particular, Gal_{4-12} arising from one and two clips were found in fractions 10−32. Evidence for the presence of Gal_9, Gal_{10}, Gal_{11}, and Gal_{12} in fractions 26, 28, 30, and 32, respectively, is shown in Figure 6. Analysis of later fractions suggested the presence of both the one- and two-clip Gal fragments up to Gal_{20}. However, at this mass range, it was difficult to categorically make the 3-amu distinction necessary to assign one versus two clips to such fragments.

Analysis of Per-O-Ethylated, Per-O-Methylated Oligoglycosylalditol Fragments. One solution to the above problem was to conduct the second alkylation step with iodoethane, resulting in ethyl (C_2H_5) rather than $C[^2H]_3$ substituents and a mass difference of 14 rather than 3 and, consequently, greater ease in distinguishing fragments generated by one clip as distinct from two clips. An added advantage of this approach is that one- and two-clip fragments containing the same number of residues, but now differing by the presence of an ethyl rather than a methyl group, could be separated by reverse-phase HPLC. The results of this analysis are presented in Table 2. The range of the Gal-containing series of fragments was now extended, and Gal_{3-23} produced by both one and two clips were generated as major products in fractions 11−36 (Table 2). There was no significant difference in peak intensities between the components of one and two clips for each of the Gal-containing series, implying a linear chain of Gal extending from a nonreducing end to at least 23 residues without any branching. This result was unexpected and required the arabinan chains, which are known to be directly attached to a 5-OH group within the galactan (Daffe et al., 1990), to be attached near its reducing end. The concept of an extended 23-unit, nonreducing end galactan is enshrined in macromotif B (Figure 5).

This approach of ethyl tagging of the per-*O*-methylated oligoglycosylalditols followed by FAB/MS screening of HPLC fractions also allowed corroboration and extension of earlier information obtained through $C[^2H]_3$ labeling on the structures of the large oligoarabinosylarabinitols (Table 2). The nonreducing-terminal (one-clip) series of Ara fragments, i.e., t-Ara_5−t-Ara_8, first emerged as major peaks in fractions 13−19, then stopped, and resumed again as t-Ara_{17-22} in fractions 28−30, although in this instance, weak one-clip Ara fragments of t-Ara_{9-16} were detected, presumably due to some arabinan heterogeneity. Due to the 14-amu differences between one- and two-clip Ara fragments, it was now possible to recognize the one-clip Ara_{22} unequivocally in contrast to the tentative assignment made earlier through $C[^2H]_3$ labeling. In addition, one-clip Ara_{23} was also clearly observed, allowing unequivocal recognition of macromotif A (Figure 5A) composed of 23 arabinosyl

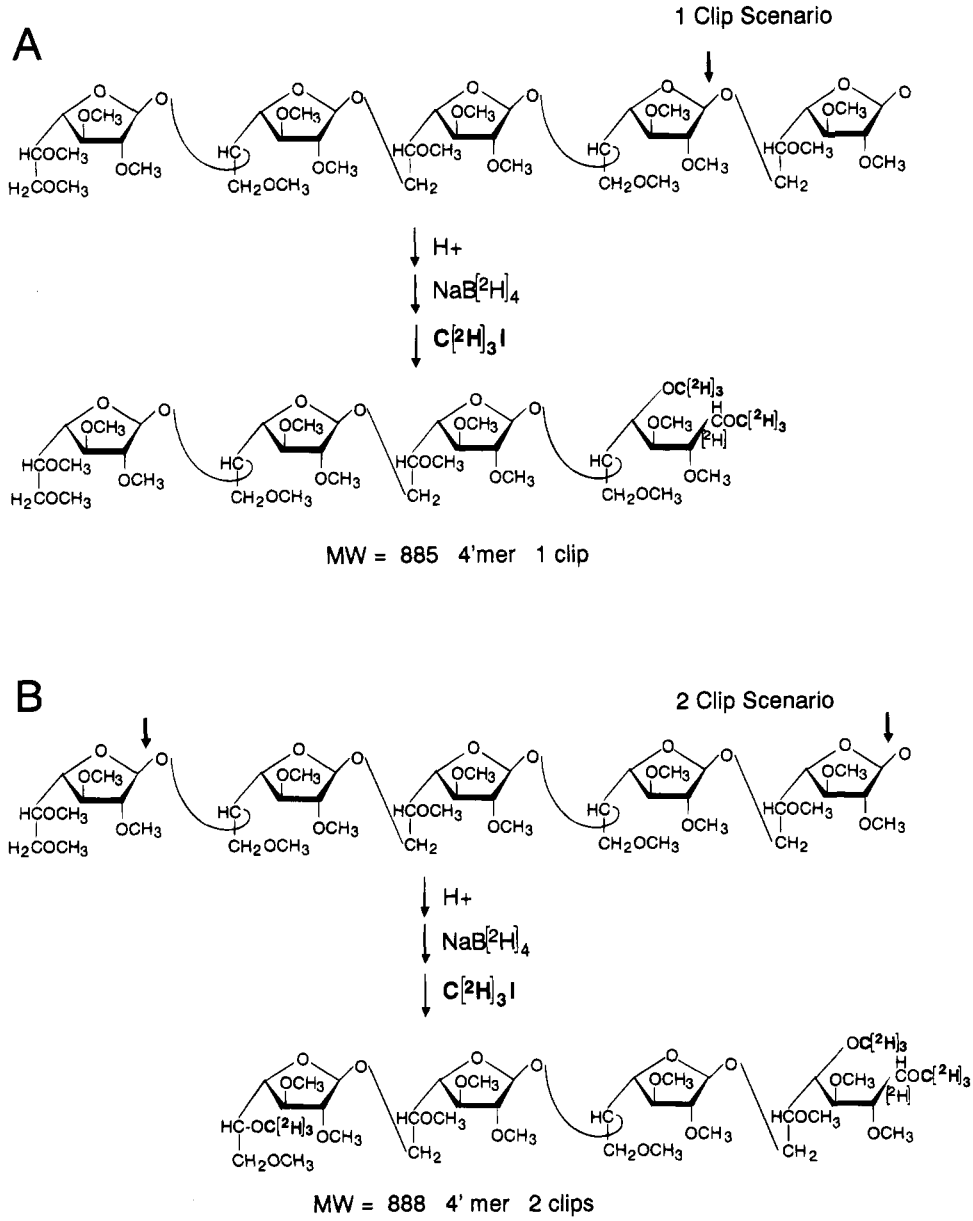

FIGURE 3: Formation of alkylated trigalactosylgalactitols (4-mers) by one (A) or two cleavages (B). The single-cleavage products can be produced only up to the point of arabinosyl branching (motif E in Figure 1). After an arabinosyl branch, the galactans would require two cleavages to release the nonreducing end.

residues. A very weak one-clip Ara_{24} was observed; however, no higher homologs of one-clip Ara were observed. Two-clip Ara fragments of up to 26 units were seen. We are inclined to attribute the presence of minor fragments, all larger than Ara_{23}, to some minor heterogeneity in the size of the arabinan chains rather than as evidence of major chain extension beyond Ara_{23} (see below). Other minor Ara signals in fractions 20−27 included those indicative of three and four clips.

Determination of the Anomeric Configuration of the L-*Rhap Residue Contained within the "Linker Unit".* Another important outcome of the present study was the definition of the anomeric configuration of the key Rha residue linking the AG heteropolysaccharide to peptidoglycan. Since the L-Rha*p* residue represents only about 1% of the total neutral sugar composition of the mAGP complex and since ^1H NMR analyses of the anomeric region are not sufficient to define Rha anomeric configurations, this question was not addressed previously (McNeil et al., 1990). The availability of gram quantities of cell wall and the ability of inverse detection NMR to derive $^{13}C-^1H$ coupling constants allowed a return to this question. The mAGP complex obtained from 2 g of *M. bovis* BCG, which was shown earlier to be identical to the mAGP complex of *M. tuberculosis* (Daffe et al., 1993), was partially hydrolyzed and reduced with sodium borohydride, and the resulting oligoglycosylalditols were per-*O*-methylated (Hakomori, 1964; Fujioka et al., 1985), partially fractionated by medium-pressure silica gel chromatography, and further resolved on a reverse-phase C-18 Sep-Pak cartridge by application of a stepwise gradient of acetonitrile in water. The 20% acetonitrile fraction contained the per-*O*-methylated alditol derivative of L-Rha*p*-(1→3)-D-GlcNAc (0.9 mg). The electron-impact mass spectrum (EI/MS) of the disaccharide [L-Rha*p*-(1→3)-D-GlcNAc] showed characteristic A-series fragments (Lonngren & Svensson, 1974; Lundblad et al., 1975): aA_1 (*m/z* 189); aA_2 (*m/z* 157); aA_3 (*m/z* 125); Ald (*m/z* 276); and the alditol cleavage ions 89, 130, 348, 392, and 436 (McNeil et al.,

Table 1: FAB/MS Analysis of the HPLC-Fractionated Partially *O*-Trideuteriomethylated, Partially *O*-Methylated Oligoglycosyl Alditols Arising from the AG of *M. tuberculosis*

HPLC fraction no.	arabinan component: no. of Ara residues (*m/z* of $[M + Na]^+$ ion)			galactan component: no. of Gal residues (*m/z* of $[M + Na]^+$ ion)	
	1 clip	2 clips	3 clips	1 clip	2 clips
10	6 (1052)			4 (908)	4 (911)
11		6 (1055)			
12	7 (1212)				
13		7 (1215)			
14		7 (1215)		5 (1112)	5 (1115)
15	8 (1372)[a]				
16		8 (1375)			
17	9 (1532)[c]	9 (1535)[c]	9 (1538)	6 (1316)[a]	6 (1319)
18	10 (1692)[c]	9 (1535)[c]	9 (1538)	5 (1316)	
19		9 (1535)	9 (1538)[a]		
20		10 (1695)[a]	10 (1698)[c]	7 (1520)[a]	7 (1523)[a]
21		11 (1855)[c]	10 (1598)[c]	7 (1520)[a]	7 (1523)[a]
22		11 (1855)[a]	11 (1858)[a]		
23		12 (2015)[c]	11 (1858)[c]	8 (1724)[a]	8 (1727)[a]
24		12 (2015)	12 (2018)	8 (1724)	8 (1727)
25		13 (2175)[a]	13 (2178)[c]	9 (1928)[b]	9 (1931)[a]
26		14 (2335)	14 (2338)	9 (1928)	9 (1931)
27		15 (2495)	15 (2498)		
28		15 (2495)[c]	15 (2498)[c]	10 (2132)[a]	10 (2135)[a]
		16 (2655)[a]	16 (2658)[c]		
29	17 (2812)[a]	16 (2655)[c]	16 (2658)[c]		
		17 (2815)[a]			
30	18 (2972)[a]	17 (2815)[b]	17 (2818)[b]	11 (2336)	11 (2339)
		18 (2975)[a]			
31	19 (3132)	19 (3135)		11 (2336)	
32	20 (3292)	20 (3295)		12 (2540)	12 (2543)
33	21 (3452)	21 (3455)		13 (2744)	13 (2747)
	22 (3612)	22 (3615)			
34				13 (2744)	
35				14 (2948)	14 (2951)
36				15 (3152)	15 (3359)
37				16 (3356)	16 (3359)
38				17 (3560)	17 (3563)
39				18 (3764)	18 (3767)
40				19 (3968)	19 (3971)
41				20 (4172)	20 (4175)

[a] Strong intensity. [b] Moderate intensity. [c] Weak intensity.

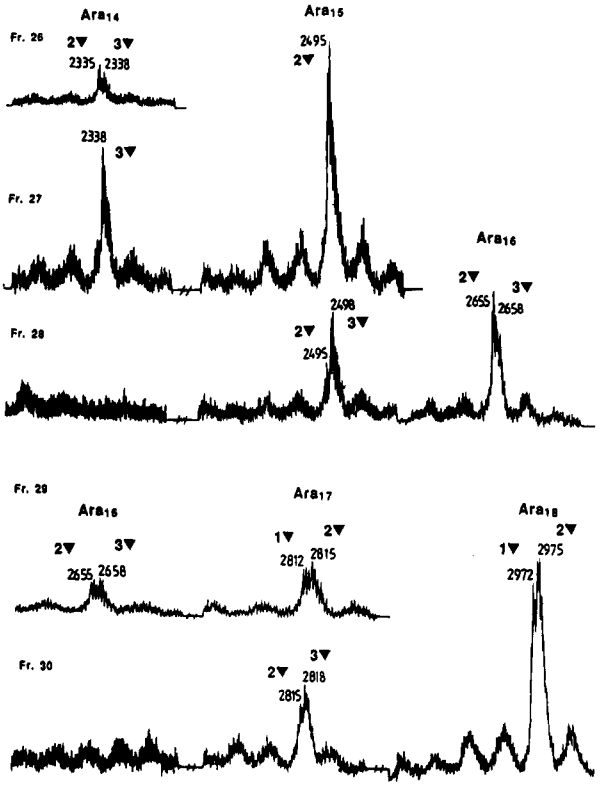

FIGURE 4: Part of the FAB/MS spectra of the partially *O*-tridetueriomethylated, partially *O*-methylated oligoarabinosylarabinitols present in HPLC fractions 26–30 demonstrating the presence of Ara_{14-18}. Fr., fraction number; 1▼, fragment produced by one clip; 2▼, fragment produced by two clips; 3▼, fragment produced by three clips.

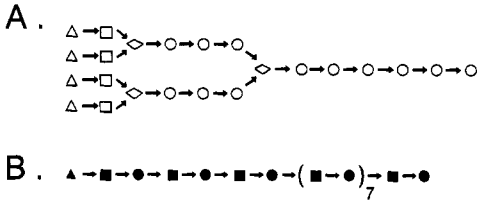

FIGURE 5: Macro structural motifs present in the arabinan (A) and galactan (B) components of AG. We propose that the entire AG molecule contains three copies of macromotif A and one copy of macromotif B. In the illustration of macromotif B, the penultimate β-Gal*f* residue is 6-linked; however, this residue may also be 5-linked. △, t-β-D-Ara*f*; □, 2-α-D-Ara*f*; ○, 5-α-D-Ara*f*; ◇, 3-5-α-D-Ara*f*; ▲, t-β-D-Gal*f*; ■, 6-β-D-Gal*f*; ●, 5-β-D-Gal*f*.

1990). Hydrolysis, reduction, and per-*O*-acetylation yielded 1,5-di-*O*-Ac-2,3,4-tri-*O*-Me-rhamnitol (*m/z* 115, 118, 131, 162, and 175) and 2-*N*-Me-2-*N*-Ac-3-*O*-Ac-1,4,5,6-tetra-*O*-Me-glucosaminitol (*m/z* 130, 246, and 290) as expected. In addition, 1,4-di-*O*-Ac-2,3,5,6-tetra-*O*-Me-galactitol as well as four or five galactitols were found that had been reduced before methylation and were only partially methylated. Difficulty in methylating 6-linked alditols had previously been encountered (Sharp et al., 1984), presumably because the free hydroxyl groups on the alditol of the mono-Gal*f* galactitols resulted in the copurification of this product with the compound of interest. Nevertheless, $^1H/^{13}C$ correlation NMR analyses (results not shown) revealed the β-D-Gal*f* ^1H NMR anomeric resonances as two broad singlets centered at 5.01 ppm which correlated to two C-1 resonances at approximately 106.9 ppm in ^{13}C NMR. Thus, the β-D-Gal*f* signals could be unambiguously assigned and did not interfere with the NMR signals of the L-Rha*p* unit. Besides the β-D-Gal*f* anomeric signals, the ^1H NMR spectrum at 300 MHz revealed the presence of two anomeric protons in an approximate ratio of 1:1 at 4.74 ppm (doublet; $J_{1,2} < 2$ Hz) and 4.84 ppm (doublet; $J_{1,2} < 2$ Hz) which are due to the H-1 of the L-Rha*p* glycosyl residue. The presence of two anomeric resonances is not clear but is probably due to hindered rotation across the $-CN(CH_3)COCH_3$ bond of the glucosaminitol residue, since hindered rotation of an amide bond substituted with an *N*-formyl group has been described among the glycopeptidolipids of the *M. avium* complex (McNeil et al., 1988). The chemical shift and coupling constants are consistent with either an α or β anomeric configuration. However, it is well established that the coupling constant between C-1 and H-1 ($^1J[^{13}CH]$) in pyranose derivatives of carbohydrates is useful in the assignment of anomeric configurations since pyranoses with an axial H-1 have a $^1J[^{13}CH]$ value which is approximately 10 Hz lower than the corresponding value in compounds with an equatorial H-1 (Bock & Pedersen, 1974). Thus, a mixutre of α- and β-tri-*O*-methylrhamnose methyl glycosides were prepared by methylation of monomeric rhamnose (Ciucanu & Kerek, 1984). The $^1J[^{13}CH]$ coupling constants of the two anomers were found to be 167 and 154 Hz and were

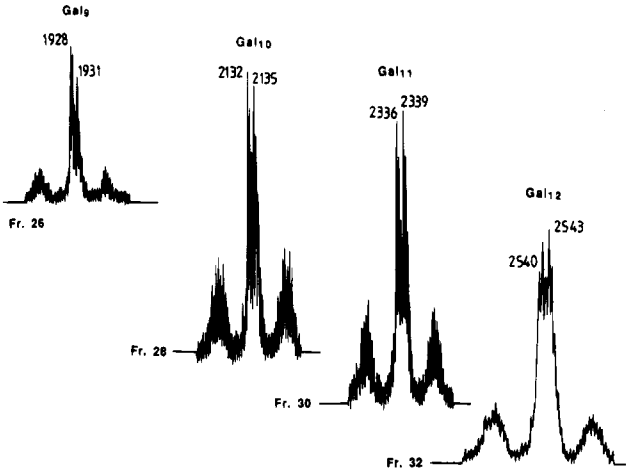

FIGURE 6: Part of the FAB/MS spectra of the partially *O*-trideuteriomethylated, partially *O*-methylated oligogalactosylgalactitols demonstrating the presence of Gal_{9-12} in HPLC fractions 26, 28, 30, and 32. All Gal signals arose from one and two clips.

thus assigned as the α and β configurations, respectively. In the case of the reduced and methylated derivative of L-Rha*p*(1→3)-D-GlcNAc, the value of 167 Hz was obtained for the $^1J[^{13}CH]$ coupling constant of both anomeric resonances at 4.74 and 4.84 ppm, allowing complete characterization of the specific diglycosyl bridge as α-L-Rha*p*-(1→3)-D-GlcNAc.

Conformational Properties of Bound Cell Wall Mycolates. Some questions concerning the conformational properties of the mycolate residues attached to the nonreducing termini of arabinan were also resolved in the present study. Previously we demonstrated that the long-chain α-alkyl-β-hydroxy mycolic acids of several *Mycobacterium* spp. were attached at the 5-position of both the terminal β-D-Ara*f* and the penultimate 2-linked α-D-Ara*f* residues. However, the question of whether the hydroxyl group of the mycolic acid was itself substituted was never addressed.

The cell walls of *M. tuberculosis*, *M. avium*, and *M. leprae* were methylated using a modified version of the Prehm (1980) procedure. The crucial question of the need for complete per-*O*-methylation was addressed by preparing alditol acetates from a sample of methylated cell walls. By comparison with authentic standards and by a combination of GC and GC/MS, the complete absence of 1,2,3,4,5-penta-*O*-CH_3CO-arabinitol and 1,2,3,4,5,6-hexa-*O*-CH_3CO-galactitol, the expected products if undermethylation had occurred, was clearly established. The per-*O*-methylated mAGP complex was degraded by alkali to release the bound per-*O*-methylated mycolic acids, and these were further methylated by phase-transfer catalysis (Dobson et al., 1985) to afford per-*O*-methylated mycolate methyl esters. Examination by TLC (figure 7) established that, in the case of *M. tuberculosis*, *M. avium*, and *M. leprae*, the mycolate methyl esters obtained from the per-*O*-methylated mAGP complex were more apolar than the corresponding mycolate methyl esters obtained from the nonmethylated mAGP. This evidence suggested that the β-hydroxy function of the mycolates in the native cell wall had become *O*-methylated under the conditions of Prehm (1980), resulting in less polar mycolates. Accordingly, the β-hydroxy functions of the *in situ* mycolic acids in the native cell wall are not acylated, in contrast to those, for instance, of the lipid A component of the O-antigenic lipopolysaccharides. To corroborate these

Table 2: FAB/MS Analysis of HPLC-Fractionated Partially *O*-Ethylated, Partially *O*-Methylated Oligoglycosyl Alditols Arising from the AG of *M. tuberculosis*

HPLC fraction no.	arabinan component: no. of Ara residues (*m/z* of $[M + NH_4]^+$ ion)[a]		galactan component: no. of Gal residues (*m/z* of $[M + NH_4]^+$ ion)	
	1 clip	2 clips	1 clip	2 clips
6	3 (589)			
7		3 (608)[b]		
8		3 (608)[b]		
9				
10				
11	4 (749)[d]		3 (721)[d]	2 (531)[d]
12				
13	5 (909)[c]	4 (763)[d]	3 (721)[d]	
14	5 (909)	4 (763)[d]		3 (735)[d]
	6 (1069)			
15	6 (1069)[c]	4 (763)[c]	4 (925)[c]	3 (735)
16	6 (1069)	4 (763)		3 (735)
	7 (1229)	5 (923)[c]		
17	7 (1229)[c]	5 (923)		
18				
19	7 (1229)	6 (1083)[c]	5 (1129)[c]	
	8 (1389)[c]	7 (1243)		
20	8 (1389)	7 (1243)[d]		
	9 (1549)	6 (1083)		
21	9 (1549)	7 (1243)[c]	6 (1333)[d]	5 (1143)
	10 (1709)	8 (1408)		
	11 (1869)			
22	10 (1709)	7 (1243)		5 (1143)[d]
	11 (1869)	9 (1563)		
23	11 (1869)	9 (1563)[c]	7 (1537)[c]	6 (1347)[c]
	12 (2029)			
24	11 (1869)	10 (1723)[c]	7 (1537)[c]	6 (1347)
	12 (2029)			
	13 (2189)			
25	12 (2029)	11 (1883)[c]	8 (1741)[c]	7 (1551)
	13 (2189)			
26	14 (2349)	11 (1883)	9 (1945)[c]	7 (1551)
	15 (2509)	12 (2043)[c]	10 (2149)	
	16 (2669)	13 (2203)[c]		
		14 (2362)		
27	15 (2509)[e]	12 (2043)	9 (1945)	8 (1755)[c]
	16 (2669)[e]	13 (2203)[c]		
	17 (2829)[e]			
	18 (2829)[e]			
28	17 (2829)[c]	14 (2363)[b]	10 (2149)[c]	9 (1959)[c]
	18 (2989)[c]	15 (2523)[c]		
	19 (3149)	16 (2683)[b]		
29	18 (2989)	16 (2683)[d]	11 (2353)[c]	9 (1959)
	19 (3149)[d]	17 (2843)[d]		10 (2163)
	20 (3309)[d]	18 (3003)		
30	20 (3309)	18 (3003)[c]	12 (2557)[d]	11 (2367)
	21 (3469)	19 (3163)[d]		
	22 (3629)	20 (3323)		
31	23 (3789)	20 (3323)	12 (2557)	11 (2367)
	24 (3949)[e]	21 (3483)[d]	13 (2761)[d]	12 (2571)
		22 (3643)		
		23 (3803)		
32		23 (3803)	14 (2965)[d]	13 (2775)[d]
		24 (3963)	15 (3169)[d]	14 (2979)
		25 (4123)		
33		26 (4283)	15 (3169)[d]	14 (2979)[d]
			16 (3373)[d]	15 (3183)[d]
			17 (3577)	
34			17 (3577)	16 (3387)[d]
			18 (3781)	17 (3591)[d]
35			19 (3985)	18 (3795)
			20 (4189)	19 (3999)
			21 (4393)	
36			22 (4597)	20 (4203)
			23 (4801)	21 (4407)

[a] Values in parentheses are the C-12 nominal molecular weights. [b] For this compound, $[M + Na]^+$ instead of $[M + NH_4]^+$ was observed. [c] Strong intensity. [d] Moderate intensity. [e] Weak intensity.

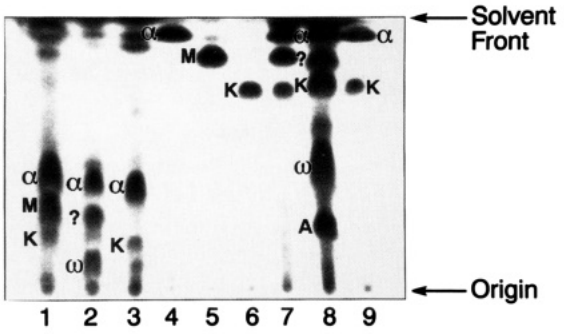

FIGURE 7: TLC of mycolate methyl esters obtained using base hydrolysis of either mAGP (lanes 1−3) or per-*O*-methylated mAGP (lanes 7−9). The mycolate esters were prepared from the following sources: lane 1 (mAGP), *M. tuberculosis*; lane 2 (mAGP), *M. avium*; lane 3 (mAGP), *M. leprae*; lane 7 (per-*O*-CH_3 mAGP), *M. tuberculosis*; lane 8 (per-*O*-CH_3 mAGP), *M. avium*; lane 9 (per-*O*-CH_3 mAGP), *M. leprae*. The mycolate methyl esters from *M. tuberculosis* (per-*O*-CH_3 mAGP) were purified and the resulting compounds were subjected to TLC in lanes 4−6: lane 4 (per-*O*-CH_3 mAGP), α-mycolate methyl ester, *M. tuberculosis*; lane 5 (per-*O*-CH_3 mAGP), methoxymycolate methyl ester, *M. tuberculosis*; lane 6 (per-*O*-CH_3 mAGP), ketomycolate methyl ester, *M. tuberculosis*. The solvent system was petroleum−ether (bp. 60−80 °C) diethyl ether (95:5 ×6). Spray, 5% ethanolic molybdophosphoric acid at 110 °C for 15 min. Abbreviations: α, α-mycolate methyl ester; M, methoxymycolate methyl ester; K, ketomycolate methyl ester; W, carboxymycolate methyl ester; A, 2-alkanol. The question mark in lanes 2 and 8 refers to the fact that the *M. avium* mycolate migrating similarly to methoxymycolate methyl esters is unidentified; it cannot be a methoxymycolate, as these compounds are not present in *M. avium*.

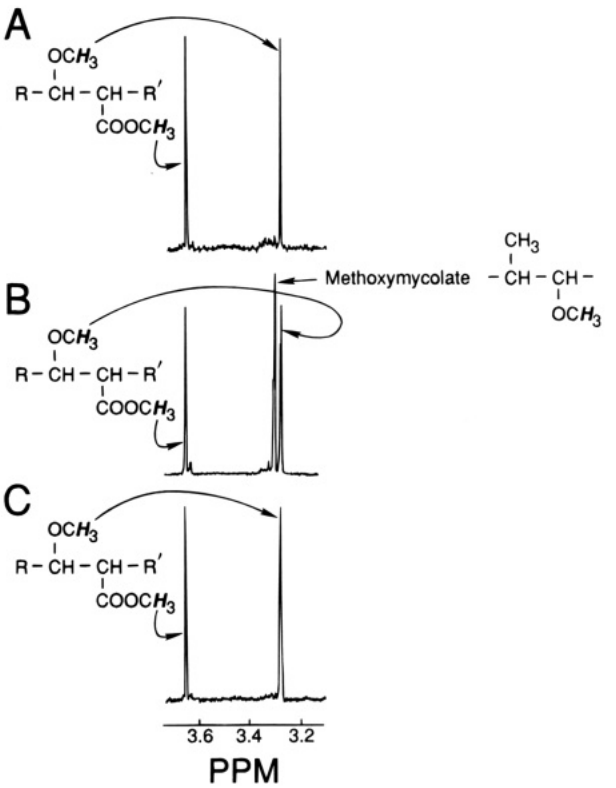

FIGURE 8: ^1H nuclear magnetic resonance spectra of per-*O*-CH_3 mycolate methyl esters from *M. tuberculosis*. (a) α-Mycolate; (B) methoxymycolate; (C) ketomycolate. Spectra were recorded at 300 MHz in $C[^2H]Cl_3$.

findings, the per-*O*-methylated mycolate methyl esters of *M. tuberculosis* (Figure 7, lane 7) were purified to afford per-*O*-methylated α-, methoxy-, and ketomycolate methyl esters (Figure 7, lanes 4−6). Analysis of the purified mycolates by ^1H NMR between δ 3.2 and 3.8 (Figure 8) revealed the appearance of an extra methoxy signal in each spectrum attributed to the "chemically induced" β-methoxy group, further supporting the principle of nonacylation of the "free" β-hydroxy group of intact cell wall mycolates.

DISCUSSION

The fine structure of the cell wall of mycobacteria is crucial to our understanding of drug and solute impenetrability (Nikaido & Jarlin, 1991), antigen processing and presentation by accessory cells (Kaufmann, 1988), and aspects of immunopathogenesis (Dannenberg, (1989). The present study confirms the presence of distinct homogalactan and homoarabinan segments within the cell wall heteropolysaccharide (Daffe et al., 1990) but also extends our knowledge by establishing the presence of two macro structural domains, one within arabinan and the other in galactan. The most informative feature was the presence of the terminal Ara_{23} mofit (Figure 5A), which means that two terminal Ara_8 units combine at a 3,5-linked α-D-Ara*f* branch point, which, in turn, is followed by six linear α-5-linked Ara*f* units. We do not insist on an exact number of 23 sugars in this enlarged motif, since weak signals indicative of Ara_{24} and beyond were observed.

A second significant feature of this latest analysis of arabinogalactan was the isolation of a terminal Gal_{23} macromotif devoid of evidence of arabinosyl branching. The obvious implication is that galactan exists primarily as a linear strand and that the arabinan(s) chains are attached close to the reducing end of the galactan, since previous methylation analyses (Daffe et al., 1990) indicated that the galactan is approximately 30 residues in length. As a consequence of these latest analyses, a revised structural model of the cell wall mAGP can be proposed (Figure 9).

The AG polymer contains approximately 100 sugar residues, 60−70 of which are Ara and 30−40 of which are Gal, based on glycosyl composition (Ara/Gal 62:35) and glycosyl linkage analysis (Ara/Gal 70:29) (Daffe et al. 1990). We had also observed 2 mol % 5,6-linked Gal*f* and had assumed that "approximately two arabinan chains are attached to the galactan core". However, the derivative (1,4-di-*O*-Ac-2,3-di-*O*-Me-5,6-di-*O*-$C_2[^2H]_5$-galactitol) is difficult to quantitate, and the figure of two could well be three, indicative of the existence of three arabinan chains, each of the 23 (or 24) macro structural motif, a theorem that is consistent with the gross sugar compositional analysis of AG. Also, we had previously estimated a content of 11 mol % 3,5-linked Ara*f* residues. However, this latest three Ara_{23-24} chain model (Figure 9) calls for nine such units. Again, given the difficulty of quantitation of the corresponding derivative, the comparative figures are not unreasonable.

The evidence for a 23-unit linear stretch of 5- and 6-linked Gal*f* residues devoid of branching dictates that the arabinan chains must be anchored close to the nonreducing terminus of galactan. Since we previously isolated the nonbranched linear →5-Gal*f*-(1→6)-Gal*f*-(1→5)-Gal*f*-(1→4)-Rha*p* unit from the reducing end of AG, it appears that the arabinan chains must emanate from a cluster of 5,6-branched Gal*f* units close to this end, probably in the region of sugar 24−27 from the nonreducing end. These considerations are contained in a revised model (Figure 9).

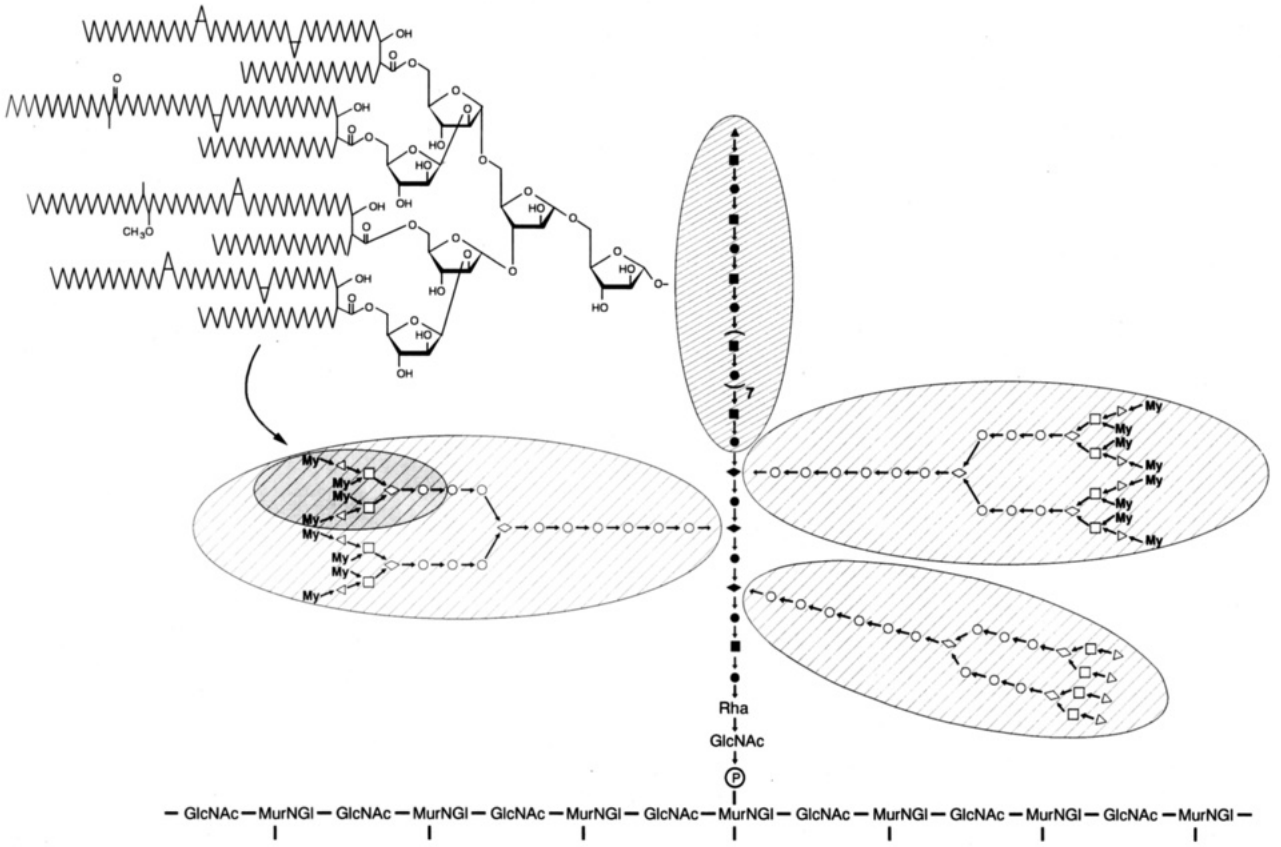

FIGURE 9: Illustration of one of the ways in which the macro structural motifs (Figure 6) of the cell wall arabinogalactan may be assembled. This is not intended to be a final representation of the structure of arabinogalactan; in particular, the details of the structure of the arabinan between macro structural motif A and the galactan are not yet known. Macromotif A, widely hatched; macromotif B, narrowly hatched; My, mycolic acid; ▽, t-β-D-Araf; □, 2-α-D-Araf; ○, 5-α-D-Araf; ◇, 3-5-α-D-Araf; ▲, t-β-D-Galf; ■, 6-β-D-Galf; ●, 5-β-D-Galf; ◆, 5,6-β-D-Galf; GlcNAc, *N*-acetylglucosamine; Rha, rhamnose; MurNGl, *N*-glycolylmuramic acid.

More importantly, these results suggest that the arabinan segments are located very close to peptidoglycan and to the cytoplasmic membrane, the presumed location of the biosynthetic and transport machinery for AG synthesis. The model further allows for an arrangement whereby the mycolic acids are added deep in the cell wall and then extend upwards to meet the capsular lipids, which is in excellent agreement with electron microscopy results (Azuma & Yamamura, 1962; Barksdale & Kim, 1977; Draper, 1982) and with recent chemical models (Minnikin, 1991).

The C-2 and C-3 centers of the mycolic acids have been shown to have an *erythro* relative configuration and 2*R*, 3*R* absolute configuration, giving rise to a stable chair conformation (Minnikin & Polgar, 1966). Consequently, the bound mycolates of the mAGP complex would favor a similar arrangement and subsequently give rise to intramolecular hydrogen bonding between the free β-hydroxy and carbonyl function of the bound mycolates. Also, it is expected that, as a result of this preferred conformation, the long alkyl chains of the mycolic acids would pack parallel to each other. Thus, the observation of the nonacylation of the β-hydroxy group supports the emerging model structures of the cell walls of mycobacteria (Minnikin, 1991; McNeil & Brennan, 1991).

The question of the acylation of the hydroxyl functions of the mycolic acids was an interesting one, brought on by comparisons with lipid A. In the absence of acylation at the 3-hydroxy position of the mycolates, it now seems likely that the roles attributed to the 3-oxymyristyl units of lipid A, namely, the provision of an extended paraffin matrix, are served by the α-branches of the mycolic acids. Indeed, a theme of a recent publication by Nikaido et al. (1993) is that the meromycolates and the α-branched chains of mycolic acids serve to provide a "staggered" monolayer which may then be complemented, respectively, by lipids with medium-chain (*ca.* C_{30}) mycocerosic acids and shorter-chain (*ca.* C_{18}) fatty acids.

ACKNOWLEDGMENT

We thank Russell Suzuki and Steve Rivoire for valuable technical assistance, Marilyn Hein for preparation of the manuscript, Carol Marander for the graphics, and Chris Rithner for the detailed NMR measurements.

REFERENCES

Abou-Zeid, C., Voiland, A., Michel, G., & Cocito, C. (1982) *Eur. J. Biochem. 128*, 363−370.
Amar-Nacasch, C., & Vilkas, E. (1970) *Bull. Soc. Chim. Biol. 52*, 145−151.
Azuma, I., & Yamamura, Y. (1962) *J. Biochem. (Tokyo) 52*, 200−206.
Azuma, I., Yamamura, Y., & Fukushi, K. (1968) *J. Bacteriol. 96*, 1885−1887.
Azuma, I., Ribi, E., Meyer, T. J., & Zbar, B. (1974) *J. Natl. Cancer Inst. 52*, 95−101.
Barksdale, L., & Kim, K. S. (1977) *Bacteriol. Rev. 41*, 217−372.
Bax, A., & Summers, M. F. (1986) *J. Am. Chem. Soc. 108*, 2093−2094.
Besra, G. S., McNeil, M., Minnikin, D. E., Porteals, F., Ridell, M., & Brennan, P. J. (1991) *Biochemistry 30*, 7772−7777.
Besra, G. S., McNeil, M., & Brennan, P. J. (1992) *Biochemistry 31*, 6504−6509.

Bock, K., & Pedersen, C. (1974) *J. Chem. Soc., Perkin Trans 2*, 293−297.
Ciucanu, I., & Kerek, F. (1984) *Carbohydr. Res. 131*, 209−217.
Daffe, M., Brennan, P. J., & McNeil, M. (1990) *J. Biol. Chem. 265*, 6734−6743.
Daffe, M., McNeil, M., & Brennan, P. J. (1993) *Carbohydr. Res. 249*, 383−398.
Dannenberg, A. M. (1989) *Rev. Infect. Dis. 11 (Suppl. 2)*, S369−S378.
Dell, A. (1990) *Methods Enzymol. 193*, 647−700.
Dobson, G., Minnikin, D. E., Minnikin, S. M., Parlett, J. H., Goodfellow, M., Ridell, M., & Magnusson, M. (1985) in *Chemical Methods in Bacterial Systematics* (Goodfellow, M., & Minnikin, D. E., Eds.) pp 237−263, Academic Press, London.
Draper, P. (1982) in *The Biology of the Mycobacteria* (Ratlege, C., & Stanford, J., Eds.), Vol. 1, pp 9−52, Academic Press, New York.
Fujioka, M., Koda, S., & Morimoti, Y. (1985) *J. Gen. Microbiol. 131*, 1323−1329.
Gerwig, G. T., Kamerling, J. P., & Vliegenthart, J. F. G. (1978) *Carbohydr. Res. 62*, 349−357.
Hakomori, S. (1964) *J. Biochem. (Tokyo) 55*, 205−208.
Hirschfield, G.R., McNeil, M., & Brennan, P. J. (1990) *J. Bacteriol. 172*, 1005−1013.
Hunter, S. W., McNeil, M., Modlin, R. L., Mehra, V., Bloom, B. R., & Brenan, P. J. (1989) *J. Immunol. 142*, 2864−2872.
Jarlier, V., & Nikaido, H. (1990) *J. Bacteriol. 172*, 1418−1423.
Kanetsuna, F. (1968) *Biochim. Biophys. Acta 158*, 130−143.
Kaufmann, S. H. E. (1989) *Curr. Opin. Immunol. 1*, 431−440.
Kotani, S., Kato, T., Matsuda, T., Kato, K., & Misaki, A. (1971) *Biken J. 14*, 379−387.
Lonngren, J., & Svensson, S. (1974) *Adv. Carbohydr. Chem. Biochem. 29*, 41−106.
Lundblad, A., Masson, P. K., Norden, N. E., Svenssen, S., & Ockerman, P. A. (1975) *Biomed. Mass Spectrom. 2*, 285−287.
McNeil, M., & Brennan, P. J. (1991) *Res. Microbiol. 142*, 451−463.
McNeil, M., Wallner, S. J., Hunter, S. W., & Brennan, P. J. (1987) *Carbohydr. Res. 166*, 299−308.
McNeil, M., Gaylord, H., & Brennan, P. J. (1988) *Carbohydr. Res. 177*, 185−198.
McNeil, M., Daffe, M., & Brennan, P. J. (1990) *J. Biol. Chem. 265*, 18200−18206.
McNeil, M., Daffe, M., & Brennan, P. J. (1991) *J. Biol. Chem. 266*, 13217−13223.
Miller, R. A., Harnisch, J. P., & Buchanan, T. M. (1984) *Int. J. Lepr. 52*, 133−139.
Minnikin, D. E. (1982) in *The Biology of Mycobacteria* (Ratledge, C., & Stanford, J., Eds.) Vol. 1, pp 95−184, Academic Press, London.
Minnikin, D. E. (1988) in *Bacterial Surface Techniques* (Hancock, I. C., & Poxton, I. R., Eds.) pp 125−136, John Wiley and Sons, Limited/Bath Press, Limited, Avon, Great Britain.
Minnikin, D. E. (1991) *Res. Microbiol. 142*, 423−427.
Minnikin, D. E., & Polgar, N. (1966) *Chem. Commun. 18*, 648−649.
Minnikin, D. E., & Goodfellow, M. (1980) in *Microbiological Classification and Identification* (Goodfellow, M., & Board, R.-G., Eds.) pp 198−250, Academic Press, London.
Minnikin, D. E., Hutchinson, I. G., Caldicott, A. B., & Goodfellow, M. (1980) *J. Chromatogr. 188*, 221−233.
Misaki, A., & Yukawa, S. (1966) *J. Biochem. (Tokyo) 59*, 511−520.
Misaki, A., Ikawa, N., Kato, T., & Kotani, S. (1970) *Biochim. Biophys. Acta 215*, 405−408.
Misaki, A., Seto, N., & Azuma, I. (1974) *J. Biochem. (Tokyo) 76*, 15−27.
Nikaido, H., & Jarlier, V. (1991) *Res. Microbiol. 142*, 437−443.
Nikaido, H., Kim, S.-H., & Rosenberg, E. Y. (1993) *Mol. Microbiol. 8*, 1025−1030.
Pessolani, M. C. V., Hunter, S. W., & Brennan, P. J. (1993) *Int. J. Lepr. 61*, 381−388.
Petit, J. F., & Lederer, E. (1984) in *The Mycobacteria: A Sourcebook* (Kubica, G. P., & Wayne, L. H., Eds.) Part A, pp 301−313, Marcel Dekker, New York.
Prehm, P. (1980) *Carbohydr. Res. 78*, 372−374.
Ratledge, C. (1982) in *The Biology of Mycobacteria* (Ratledge, C., & Stanford, J., Eds.) Vol. 1, pp 55−93, Academic Press, London.
Sharp, J. K., McNeil, M., & Albersheim, P. (1984) *J. Biol. Chem. 259*, 11321−11336.
Stacey, M., & Kent, P. W. (1948) *Adv. Carbohydr. Chem. 3*, 311−336.
Styblo, K. (1989) *Rev. Infect. Dis. 11*, S339−343.
Vilkas, E., Amar, C., Markovits, J., Vliegenthart, J. F. G., & Kamerling, J. P. (1973) *Biochim. Biophys. Acta 297*, 423−435.

BI942293C